This is a preprint, the final version is subject to change, of the American Mineralogist (MSA)
Cite as Authors (Year) Title. American Mineralogist, in press.
(DOI will not work until issue is live.) DOI: http://dx.doi.org/10.2138/am-2017-5792CCBY

REVISION 3

Spin orientation in solid solution hematite-ilmenite

Erik Brok[2, 3, 4, 5], Cathrine Frandsen[2], Kim Lefmann[6], Suzanne McEnroe[7], Peter Robinson[7], Benjamin P. Burton[8] Thomas C. Hansen[9] and Richard Harrison[1]

[1]Department of Earth Sciences, University of Cambridge, Downing Street, Cambridge CB2 3EQ, U.K.

[2]Department of Physics, Technical University of Denmark, DK-2800, Kongens Lyngby, Denmark

[3]Center for Electron Nanoscopy, Technical University of Denmark, DK-2800, Kongens Lyngby, Denmark

[4]Center for Neutron Scattering, National Institute of Standards and Technology, MD-20899, Gaithersburg, USA

[5]Department of Materials Science and Engineering, University of Maryland, MD-20742, College Park, USA

[6]Nano-Science Center, Niels Bohr Institute, University of Copenhagen, Universitetsparken 5, DK-2100 Copenhagen Ø, Denmark

[7]Geological Survey of Norway, N-7491 Trondheim, Norway

[8]Materials Measurement Laboratory, National Institute of Standards and Technology, MD-20899, Gaithersburg, USA

[9]Institut Max von Laue Paul Langevin, F-38042 Grenoble 9, France

Abstract

The spin orientation in synthetic hematite-ilmenite samples and in a sample of natural hematite was studied from room temperature to above the antiferromagnetic-paramagnetic phase transition (the Néel temperature; $T_N \approx 600 - 950$ K) by neutron powder diffraction and at room temperature by Mössbauer spectroscopy. The usually assumed magnetic structure of hematite within this temperature range is antiferromagnetic with the spins confined to the basal plane of the hexagonal structure, however, an out-of-plane spin component is allowed by the symmetry of the system and has been observed in recent studies of synthetic hematite samples. We find the spins in the antiferromagnetic sublattices to be rotated out of the basal plane by an angle between 11(2)° and 22.7(5)° in both synthetic hematite-ilmenite samples and in the natural hematite sample. The spin angle remains tilted out of the basal plane in the entire temperature range below the Néel temperature and does not depend systematically on Ti-content. The results indicate that the out-of-plane spin component is an intrinsic feature of hematite itself, with an origin not yet fully understood, but consistent with group theory. This represents a major shift in understanding of one of the two main mineral systems responsible for rock magnetism.

Keywords: Hematite, magnetic properties, spin orientation, neutron scattering, Mössbauer spectroscopy

Introduction

The ilmenite-hematite [xFeTiO$_3$-(1-x) Fe$_2$O$_3$] solid solution series has been studied extensively because of its complex and interesting magnetic and electronic properties. Intermediate compositions are magnetic semiconductors (Ishikawa and Akimoto 1957, Ishikawa 1958) and could conceivably be utilized in spintronics devices (Butler et al. 2003; Fujii et al. 2004). The FeTiO$_3$ -

Fe_2O_3 solid solution series further serves as a model system for natural ilmenite-hematite minerals, which are studied because of their remarkable magnetic properties and because of their importance as a source of anomalies in the magnetic field of the Earth (McEnroe et al. 2001; Kletetschka et al. 2002), and possibly of other planets like Mars (McEnroe et al. 2004). Interesting magnetic properties of natural hemo-ilmenite samples include giant exchange bias (McEnroe et al. 2002, 2007; Robinson et al. 2002; 2004; Fabian et al. 2008) and large and stable remanent magnetization that cannot be explained by the individual properties of hematite and ilmenite alone (Robinson et al. 2002, 2004). There is strong evidence that these properties are associated with fine scale exsolution structures observed in natural hematite-ilmenite samples (Robinson et al. 2002; Fabian et al. 2008; Brok et al. 2014). Solid solution $FeTiO_3$ - Fe_2O_3 does not exhibit these well-developed exsolution structures and can therefore be used as a baseline for determining if the observed properties are tied to the exsolution structure.

Between the Néel temperature of $T_N \approx 955$ K (Morrish 1994) and the Morin temperature of $T_M \approx 264$ K (Besser et al. 1967; Morin 1950) hematite is a canted antiferromagnet with Fe^{3+} spins aligned ferromagnetically within the basal plane of the hexagonal structure while spins in adjacent planes are aligned antiferromagnetically apart from a small canting of about 0.065° that gives rise to a small net magnetization. The spin orientation is usually assumed to be in or very close to the basal plane (Morrish 1994, Shull et al. 1951) even though the symmetry of the structure allows for an out-of-plane spin component (Dzyaloshinsky 1958). At T_M hematite undergoes the so-called Morin transition in which the spins rotate 90° to form a perfectly antiferromagnetic structure (no canting) with spins in the two sublattices parallel and antiparallel to the hexagonal [001] axis. The Morin transition is known to be suppressed by impurities as well as by finite crystallite size and the canted antiferromagnetic structure with spins close to the basal plane is maintained even at the lowest

temperatures in nanoparticles smaller than 20 nm and in samples doped with even small amounts (<1%) of Ti (Bødker et al. 2000; Besser et al. 1967; Morrish 1994).

In a natural sample of ilmeno-hematite with nanoscale exsolution lamellae of ilmenite in the parent hematite structure Harrison et al. (2010) found the spins to be rotated 29.5° out of the basal plane and in a nanocomposite of hematite particles interacting with particles of NiO Frandsen et al. (2011) measured an out-of-plane angle as large as 70°. These experiments show that exchange interaction across interfaces can change the spin orientation in hematite. In studies of Al-substituted hematite it has been proposed that intermediate structures (spins not parallel or perpendicular to [001]) exist close to the Morin transition (Vandenberghe 2001, 2002). Even in pure hematite at ambient conditions out-of-plane spin-angles of about 18° have been measured by Parise et al. (2006) and Klotz et al. (2013). The spin orientation in hematite between T_M and T_N is thus not always confined to the basal plane. The spin orientation could depend on factors such as impurities and strain and could thus be sample dependent. In particular, the spin orientation in Ti-substituted hematite could deviate from that of pure hematite, and may potentially vary with Ti-content.

The degree of Fe-Ti cation order in hematite-ilmenite solid solutions depends greatly on the composition and thermal history of the sample. Quenched samples containing less than approximately 40% ilmenite exhibit no long-range Fe-Ti cation order, and adopt the space group R-3c. Quenched samples containing more than approximately 40% ilmenite exhibit an increasing degree of short- and then long-range Fe-Ti cation order with increasing ilmenite content, leading to a loss of symmetry from R-3c to R-3 (Harrison and Redfern 2001). Quenched samples with intermediate compositions are infamous for their ability to acquire self-reversed thermoremanent magnetisation, linked to chemical and ordering heterogeneities at the nanoscale (Fabian et al. 2011; Robinson et al. 2011, 2012, 2014).

Here we investigate the spin-orientation in synthetic samples of solid solution [xFeTiO$_3$-(1-x) Fe$_2$O$_3$] with compositions x ≤ 0.40 and in a natural hematite sample (x = 0). We use Rietveld refinement of neutron powder diffraction data, taken at temperatures from room temperature to T_N, to determine the average out-of-plane spin angle α. We use Mössbauer spectroscopy to investigate the distribution of α in each sample. We find that the spins in all hematite-ilmenite samples have significant out-of-plane components in the range from α = 11(2)° to α = 22.7(5)°. All given uncertainties are the estimated standard deviations (σ). Even the natural hematite sample has a significant out-of-plane spin-angle of α = 18.1(6)°. Our results show that α does not vary systematically with Ti-content.

Group theory and crystallography

Magnetic ordering in hematite at temperatures $T_M < T < T_N$ can be described by a two-dimensional primary magnetic order parameter (Q_1, Q_2) corresponding to the active irreducible representation (mΓ_3^+) of the parent space group (R-3c). Different combinations of Q_1 and Q_2 lead to three possible magnetic space groups: C2/c for $Q_1 \neq 0$, $Q_2 = 0$; C2'/c' for $Q_1 = 0$, $Q_2 \neq 0$; and P-1 for $Q_1 \neq 0$, $Q_2 \neq 0$. The magnetic structure observed by experiment is the C2/c structure with $Q_1 \neq 0$ and $Q_2 = 0$. This structure is a canted antiferromagnet with parallel alignment of the spins within each (001) layer and nearly antiparallel alignment of spins in neighboring (001) layers (indices refer to the parent hexagonal unit cell). The primary order parameter Q_1 places spins parallel to the (001) basal plane and nearly perpendicular to the diad (i.e. nearly perpendicular to an a crystallographic axis of the parent hexagonal unit cell). A degree of canting within the basal plane is permitted by the C2/c symmetry, such that spins are rotated by ~0.065° to create a weak ferromagnetic (WF) moment along the diad (Morrish 1994). A secondary irreducible representation (mΓ_1^+) is permitted within C2/c. By itself, mΓ_1^+ would give a strictly antiferromagnetic alignment of spins normal to the

(001) basal plane (as observed for $T < T_M$). In combination with $m\Gamma_3^+$, the antiferromagnetic spins are rotated about the diad so that they lie at an angle, α, to the basal plane, as has been observed in recent experiments (Frandsen et al. 2011; Harrison et al. 2010; Klotz et al. 2013; Parise et al. 2006). Note that even when $\alpha \neq 0$, the canted WF moment still lies parallel to the diad and therefore in the basal plane. If we assign a secondary order parameter Q_3 to $m\Gamma_1^+$, then Q_1 and Q_3 are proportional to the in-plane and out-of-plane spin components, respectively. Given the symmetry relationship between Q_1 and Q_3, it is permitted for these order parameters to couple bilinearly in the expansion of Gibb's free energy. In this case we would expect that Q_3 would vary linearly with Q_1. This proposition can be tested directly by Rietveld refinement of high-temperature powder neutron diffraction data.

Here we follow the crystallographic conventions and refinement procedures described in detail by Harrison et al. (2010). For technical reasons, refinements were performed in a non-standard *A2/a* setting of the monoclinic *C2/c* phase described above. For ease of comparison with the high-temperature hexagonal phase the unit cell parameters are presented here using a monoclinic pseudocell with volume equal to that of the high-temperature hexagonal cell: $a_m = (1/\sqrt{3})[210]_{hex}$, $b_m = [010]_{hex}$, $c_m = [001]_{hex}$, $\beta_m \sim 90°$, where $[abc]_{hex}$ refers to the axes of the hexagonal cell. Similarly the refined magnetic moments M_x and M_y in the monoclinic cell are converted to components parallel ($M_{\parallel}$) and perpendicular ($M_{\perp}$) to the basal plane. Figure 1 shows a representation of the chemical and magnetic structure of hematite with a spin rotation of $\alpha = 20°$ away from the basal plane.

Methods

Samples

Synthetic powder samples of [xFeTiO$_3$-(1-x) Fe$_2$O$_3$] with nominal compositions of x = 0.13, 0.20, 0.35 and 0.40 were prepared by heating in sealed silica tubes followed by rapid cooling of mixtures of Fe_2O_3 and TiO_2 as described in Burton et al. (2008). A natural sample of hematite was obtained from the Sedgwick Museum of Earth Sciences, Cambridge, United Kingdom. The hematite sample was crushed and ground into a fine powder. We refer to these samples as ilm13, ilm20, ilm35, ilm40 and hem.

Neutron powder diffraction

We performed neutron powder diffraction experiments at the OSIRIS instrument at the ISIS spallation neutron source, Oxfordshire, UK and at the D20 instrument at the reactor source at Institut Laue Langevin, Grenoble, France. In both experiments the samples were mounted inside an evacuated furnace providing a temperature range from room temperature to 1373 K (1100 °C). The Néel temperatures of the Ti-containing samples are expected to be lower (Besser et al. 1967) than the 955 K of pure hematite, and the available temperature range should thus allow us to obtain diffraction patterns from hundreds of degrees below, to well above the magnetic phase transition. The samples were loaded in vanadium cylinders with thin walls to minimize contamination from the sample holder in the diffraction patterns.

We collected neutron diffraction patterns for the samples hem, ilm20, ilm35 and ilm40 at the OSIRIS instrument at ISIS. OSIRIS is a time-of-flight indirect geometry spectrometer/diffractometer with a ring of detectors for diffraction placed around the incident beam covering a range of scattering angles $150° < 2\theta < 171°$. The accessible d-spacing range is from 0.8 Å to 20 Å with optimal d-spacing resolution $\frac{\Delta d}{d} = 2.5\times10^{-3}$. With choppers running at a 25 Hz frequency, a 4 Å wide wavelength range with minimal contamination of higher order neutrons is allowed to reach the sample. To obtain one diffraction pattern we perform 4 measurements with

different relative phasings of the choppers in order to change the incoming wavelength range and thus span the desired range of *d*-spacings. The four measurements are combined to a diffraction pattern that continuously covers *d*-spacings from approximately 0.72 Å to approximately 5.25 Å.

We obtained neutron diffraction patterns of the sample ilm13 at the high-flux powder diffractometer D20 at the ILL. The HOPG(002) monochromator with a take-off angle of 42° and the detector, covering 153.6° in 2θ , provided us with neutrons of a wavelength of 2.4 Å and a *d*-spacing range of 1.3 Å -13.1 Å with a resolution on the order of $\frac{\Delta d}{d} = 10^{-2}$.

While the resolution of D20 is inferior to that of OSIRIS, the high flux at D20 enabled us to measure a diffraction pattern in a few minutes. It was therefore possible to measure a temperature series of closely spaced data points (in steps of about 5 K) from room temperature to far above the Néel temperature of the sample (≈ 800 K) within one day.

Rietveld refinements

To obtain the out-of-plane spin-angle α from the diffraction patterns taken below T_N, Rietveld refinements were performed using the monoclinic model of hematite in the space group A112/a, as described in Harrison et al. (2010), using the GSAS program (Larson and von Dreele (1994)). The background was modeled with Chebyshev polynomials and the peak profile with appropriate peak shape functions for Time-of-flight (OSIRIS) and constant wavelength (D20) data. In all refinements the cations were assumed to be fully disordered. The validity of the assumption of cation disorder can be verified by the absence of reflections from the *R-3* structure of $FeTiO_3$ in the diffraction data. Long-range cation order would give rise to a nonzero intensity at the position of the magnetic hematite peaks above T_N which was not observed.

For all samples, small peaks in the diffraction patterns were identified as belonging to the structure of magnetite. Because of this magnetite impurity, a magnetite phase was added to the refinements for ilm20 and hem where the impurity peaks were most pronounced. Magnetite was refined as a both nuclear and magnetic phase in the *R-3m* space group. Only a scale factor, the size of the magnetic moment, and unit cell parameters were refined. The results from refinement of the magnetite structure are not expected to be very accurate or useful since this is just a minor impurity phase. For the other samples the magnetite content was so small that it was not necessary to include in the refinements.

When refining data from temperatures close to T_N it was sometimes necessary to reduce the number of refined parameters, or to use Marquardt-damping to achieve convergence in the refinements.

Refinement of the atomic occupation factors produced unrealistically small values compared to the nominal compositions. Instead an initial refinement of room temperature diffraction data was performed for each sample using the nominal composition. The compositions (and thus the atomic occupation factors for Fe and Ti) were then determined from the refined unit cell volume using the formula (Harrison 2010)

$$V = 1.685\,x^2 + 10.823\,x + 301.740 \quad (x < 0.5), \qquad (1)$$

where V is the volume of the hexagonal unit cell in $Å^3$. The occupancies were then fixed at the values obtained for the respective sample in each refinement.

In the D20 experiment we measured a large number of diffraction patterns of ilm13 above T_N. This high temperature data was refined to the high-symmetry hexagonal unit cell and with zero magnetic moment. At high temperatures (≈ 1100 K) we observed that diffraction lines from magnetite grew in intensity, probably because of conversion of hematite to magnetite, and we

therefore added a magnetite phase in the refinements for the highest temperatures. Because of the conversion to magnetite the sample composition may change and the unit cell parameters can therefore be expected to change at these high temperatures.

The uncertainties given on parameters from the Rietveld refinements are the estimated standard deviations produced by GSAS or calculated from these using standard error propagation methods.

Mössbauer spectroscopy

^{57}Fe Mössbauer spectroscopy measurements at room temperature were performed on samples hem, ilm20, ilm35 and ilm40. To prepare Mössbauer-absorber samples a small amount of the sample was ground to a fine powder in an agate mortar and approximately 30 mg of it was mixed with boron nitride and placed in a plastic holder. The Mössbauer spectra were obtained at Department of Physics, Technical University of Denmark, Kgs. Lyngby, Denmark using a constant acceleration Mössbauer spectrometer with a source of ^{57}Co in rhodium. The magnetically split spectra were fitted to sextets of Lorentzians with pairwise common line width of lines 1 and 6, 2 and 5, and 3 and 4. The area ratio between lines 1 to 6 was constrained to 3:2:1:1:2:3. The Mössbauer spectrometers were calibrated with a foil of α-Fe at room temperature and the isomer shifts are given relative to this calibration value.

Results

Neutron powder diffraction

The room temperature diffraction patterns from the samples hem and ilm13 are shown in Figure 1. The positions of the (101) and (003) magnetic peaks and the most intense of the peaks

from the magnetite impurity are indicated. The much better resolution in the data from OSIRIS as compared to D20 is clearly seen by comparing the width of the peaks in the two diffraction patterns. The refined model represents the data reasonably well, and the disagreements between model and measurement originate primarily from misfits of the peak profiles, which is a problem that can never be completely eliminated. There was some variation in background between samples and in some cases the background was somewhat nonuniform and not that well modeled. However, it is important to note that for all samples the background was well modeled in the *d*-spacing range close to the two main magnetic peaks (101) and (003), which is the area of the diffraction pattern that is most significant for obtaining information about the magnetic structure about the sample, in particular the out-of-plane spin-angle α.

A three-dimensional representation (*d*-spacing, temperature, intensity) of the complete set of measurements of the ilm13 sample from room temperature (295 K) to above 1240 K is displayed in Figure 2. The magnetic phase transition is identified by the disappearance of the two main magnetic peaks ((101) at $d \approx 4.2$ Å and (003) at $d \approx 4.6$ Å) at a temperature of approximately 800 K. The weak line at $d \approx 4.9$ Å can be identified as a magnetic reflection from magnetite and it completely disappears at the Curie temperature of magnetite (≈ 850 K). Lines pertaining to the magnetite crystal structure can also be identified (e.g. at $d \approx 3.0$ Å) and these achieve a significant gain in intensity at temperatures around 1100 K, indicating that in addition to a small initial impurity of magnetite part of the sample is being reduced to magnetite during heating. When magnetite is produced by reduction of the sample the composition of the remaining hematite-ilmenite becomes more Ti-rich resulting in an enlargement of the unit cell seen as a shift of the diffraction lines to lower scattering angles (larger *d*-spacings).

The refined unit cell volumes and the determined compositions are given in Table 1 together with the room temperature values of the magnetic moments $M_{\parallel}$, $M_{\perp}$, M_{tot} and α. The compositions

deviate in some cases from the nominal values. In all cases $M_{\parallel}$ is significantly larger than $M_{\perp}$, as expected for hematite between T_M and T_N. However, there is a significant out-of-plane moment for all samples. The size of α varies from 11(2)° for ilm13 to 22.7(5)° for ilm35 and it does not depend systematically on Ti-content. For the hem sample α = 18.1(6)°.

In Figure 3 we show $M_{\parallel}$, $M_{\perp}$ and the total moment M_{tot} as function of temperature for the samples hem, ilm13, ilm20 and ilm35. As the temperature increases towards T_N both components of the moment decrease at the same rate until close to T_N. For the ilm13 and ilm20 samples $M_{\perp}$ becomes zero before $M_{\parallel}$, indicating a reorientation of the spins close to T_N. However, the relative uncertainties on the refined moments (especially $M_{\perp}$) become very large close to T_N because the magnetic peaks are weak. The Néel temperatures determined from fitting the M_{tot} data to a power law $M = M_0 \left(\frac{T_N - T}{T_N}\right)^{\beta}$ are given in Table 2. The fits represent the data well until very close to T_N where the order parameter is expected to deviate from the power law because of critical behavior of the system. Because of the critical behavior a finite intensity remains in the magnetic peaks at temperatures a few K above the fitted T_N. The critical exponent β determined from the fit to M_{tot} was in the range 0.3-0.4 for all samples which is in the expected range for a phase transition in a 3-dimensional system.

In Figure 4 (left) the total moment is displayed as function of the reduced temperature (T/T_N) for all samples. In Figure 4 (right) the out-of-plane tilt angle α is displayed as a function of the reduced temperature. There is no systematic dependence of α on the Ti-concentration. The spin reorientation towards the basal plane with increasing temperature is systematic for all Ti-containing samples with the exception of two points very close to T_N ($0.995\ T_N < T < T_N$) for the ilm35 sample. The figure also illustrates that the uncertainty on α becomes large near T_N. For sample hem

there is a significant change in α between the first and the second point, which are measured at room temperature and at 673 K (400 °C) respectively.

To illustrate the relationship between the primary order parameter Q_1 and the secondary order parameter Q_3, $M_\perp$ is plotted against $M_\parallel$ in Figure 5. For the hem sample the linear fit represents the data well. For the ilm13 and ilm20 sample $M_\perp$ turns to zero before $M_\parallel$ ending the linear relationship between Q_1 and Q_3 shortly before T_N. For ilm35 the trend is the same as for the other Ti-containing samples if the three anomalous points closest to T_N are disregarded from the fit.

In the experiment at D20 on sample ilm13 we obtained sufficient data above and below T_N to follow the transformation of the monoclinic unit cell to the high-symmetry hexagonal cell occurring simultaneously with the magnetic phase transition. The change in the unit cell parameters as a function of temperature can be seen in Figure 6. The unit cell parameters for the low-temperature monoclinic phase, a_m, b_m and c_m are given in the reference frame of the monoclinic pseudo-cell and can thus be compared directly to the unit cell parameters of the high-temperature hexagonal cell, a_h and c_h. As the temperature increases a_m, and b_m converge towards the value of a_h at T_N. The slope of the curve does not change significantly at the phase transition, indicating that the strain associated with the phase transition is small. The same is true for the transformation of c_m to c_h. At high temperatures (above 1000 K) the slope of the a_h and c_h curves change. This change happens in the same temperature range where the intensity of the magnetite lines start to increase (see Fig. 2) and is probably associated with the reduction of some of the ilm13 to magnetite and the resulting change in hematite-ilmenite composition. The transformation of the crystallographic β-angle from monoclinic $\beta_m \neq 90°$ to hexagonal $\beta_h = 90°$ can be followed in Figure 7. At room temperature β_m is 90.039(7)°. As the temperature increases β_m decreases towards 90°.

Mössbauer spectroscopy

The Mössbauer spectra of the hem, ilm20, ilm35 and ilm40 samples are shown in Figure 8. Also shown are model fits to the data.

Hematite sample. The spectrum of the hem sample consists of a well-defined sextet as expected for pure hematite, as well as a small component (10 % of the spectral area) that can be ascribed to the magnetite impurity, also observed in the neutron data. The room temperature Mössbauer parameters of the hematite sextet are: Hyperfine field B_{hf} = 51.50(2) T, isomer shift *IS* = 0.370(4) mm/s and quadrupole shift ε = -0.094(4) mm/s independent of whether the magnetite impurity is included in the fit. Here the uncertainties on the hyperfine parameters are estimated from the uncertainties on the calibration with respect to α-Fe. The Lorentzian linewidths are 0.311 mm/s, 0.288 mm/s, and 0.249 mm/s for lines 1 and 6, 2 and 5, and 3 and 4 respectively. Because the linewidhts are close to the natural linewidth of 0.260 mm/s fitting with a more complicated model with a distribution of hyperfine parameters is not justified.

The quadrupole shift (ε) in the Mössbauer spectrum of hematite is sensitive to α, and the fact that the spectrum is well fitted with one symmetric sextet rather than two sextets with different ε indicates that the directions of the Fe^{3+} spins in the sample are grouped around one value of α, rather than being distributed into distinct domains with different spin-orientations. In particular, we can rule out a scenario with significant proportions of the spins being in the basal plane and along the c-axis respectively. In principle the average value of α can be found from the quadrupole shift of the spectrum from (Morrish 1994)

$$\varepsilon = \varepsilon_0(3\cos^2(90° - \alpha) - 1)/2, \quad (2)$$

where ε_0 depends on the quadrupole moment of the iron nucleus in the nuclear spin= 3/2 state, and on the electric field gradient along the c-axis. From the literature (Artman et al. 1968, Tobler et al.

1981) ε_0 can be estimated to $\varepsilon_0 = 0.215(5)$ mm/s and α can be determined from the measured quadrupole shift -0.094(4) mm/s to be $\alpha = 12(2)°$.

Mössbauer spectra of the hem sample were also collected at 80 K and 20 K (not shown). These spectra taken below T_M have quadrupole shifts of 0.190(4) mm/s and 0.189(4) mm/s respectively, corresponding to an imperfect Morin transition with the spins making an angle of 16(2)° with [001] even at 20 K.

Ti-containing samples. The room temperature Mössbauer spectra of the samples ilm20, ilm35 and ilm40 have much broader lines than the hem spectrum. Each spectrum is fitted with four sextets, three with isomer shifts close to 0.4 mm/s, corresponding to Fe^{3+}, and one with isomer shift closer to 0.6 mm/s, corresponding to Fe^{2+}. The hyperfine fields of the Fe^{3+} sextets are in the range 47 T - 50 T and thus a bit lower than expected for pure hematite at room temperature (probably due to Ti^{4+} substitution in the hematite structure). The hyperfine field of the Fe^{2+} sextet is 37 - 44 T in all samples. The quadrupole shifts of the Fe^{3+} sextets are in the range between -0.110 mm/s and -0.076 mm/s. The ilm35 spectrum contains a central doublet with isomer shift 0.377(4) mm/s and quadrupole splitting 0.663(4) mm/s, suggesting that it could originate from a paramagnetic Fe^{3+} phase. The quadrupole shifts in the Ti-containing samples cannot be used to calculate α from Equation (2) because ε_0 depends on the electric field gradient along the hexagonal c-axis, which is expected to change when Ti is substituted for Fe in the hematite structure. While it is not possible to calculate α the fact that the quadrupole shifts of all the Fe^{3+} sextets are close to -0.1 mm/s suggests that, like in the hem sample, the spin orientations are grouped around some average angle, rather than two distinct populations of in-plane and out-of-plane spins. The room temperature hyperfine parameters obtained from the sextet fits can be seen in Table 3.

Discussion

The Rietveld refinement of the neutron powder diffraction data tells us that there is a significant out of plane component of the hematite spins in all hematite-ilmenite samples and even in the natural hematite sample. While there is a variation in the measured α between samples it does not seem to depend systematically on Ti-content. There is no pronounced temperature dependence of α, however, for the Ti-containing samples the spins tend to reorient towards the basal plane close to T_N, with the exception for a few points very close to T_N for ilm35. It should be noted that very close to the phase transition the refinement of the magnetic structure is susceptible to systematic errors and the parameters extracted from the refinements should not be given too much weight.

From the quadrupole shift in the room temperature Mössbauer spectrum of the hem sample the spin-angle can be determined to $\alpha = 12(2)°$, which is not consistent with the neutron result ($\alpha = 18.1(6)°$), although it does confirm that there is a significant out of plane component of the spin in the natural hematite sample. The value of α determined from the quadrupole shift in the Mössbauer spectrum may not be taken as an accurate number because the hyperfine parameters (most importantly ε_0) may depend delicately on crystallographic strain and other sample dependent factors such as impurities in the structure. Because of this uncertainty in the determination of α from Mössbauer spectroscopy we regard the value obtained with neutron diffraction as more accurate. From the Mössbauer spectrum taken at 20 K we find the spins to be rotated by 16(2)° from the *c*-axis. As soon as the spins are observed to be rotated away from the *c*- axis, a canted moment becomes symmetry-allowed and could contribute to the defect moment sometimes observed for hematite below T_M. The spectrum also reveals that the spin orientation is not grouped in distinct populations, e.g. one with $\alpha = 0°$ and one with $\alpha = 90°$ corresponding to the spin orientation usually assumed above and below the Morin transition, but are grouped around some

average value. The Mössbauer spectra of ilm20, ilm35 and ilm40 suggest that this is the case also in Ti-substituted hematite.

We followed the structural phase transition at T_N for a sample (ilm13) with $x = 0.176(12)$ and observed a gradual transition from the low symmetry monoclinic cell to the high symmetry hexagonal cell. Within the resolution of D20 there is no strain associated with the phase transition.

The 30° out-of-plane spin-angle found by Harrison et al. (2010) was believed to be linked to the exsolution microstructure in the natural sample, and it is surprising that we find appreciable out-of-plane spin-angles in our samples that should not exhibit pronounced exsolution microstructure. While the neutron diffraction data exclude a long range ordering of the Ti-cations it is not possible to determine whether some short-range cation ordering exists. Frandsen et al. (2010) suggested that small clusters of ordered hematite exist inside an ilmenite matrix for samples with $x > 0.5$. They conclude that the size of the hematite clusters is only on the order of 1-2 nm. Spins around the interfaces of such clusters could be rotated due to exchange interaction between Fe^{2+} and Fe^{3+} species. This would, however, not explain why we observe an out-of-plane spin orientation in the natural hematite sample. The out-of-plane spin angle of 30° observed by Harrison et al. (2010) is significantly larger than the spin angles we find in our samples. This suggests that while some out-of-plane spin orientation may be intrinsic to the hematite magnetic structure exsolution could enhance the effect.

It is well known that the magnetic structure of hematite does not prohibit an out-of-plane spin-component, however, it is generally assumed to be much smaller than the $18.1(6)°$ found in this work (Dzyaloshinsky 1958). The spin orientation in hematite above and below the Morin transition is determined by a fine balance between competing anisotropies that may depend on factors such as impurities, strain and applied pressure (Morrish et al. 1963, Artman et al. 1965;

Besser 1967; Klotz et al. 2013). In numerous neutron studies it has been observed that there is a finite intensity in the magnetic (003) reflection at temperatures far below the Morin transition (Morrish 1963; Krén et al. 1974; Sváb and Krén 1974; Morrish 1994), proving that the spins are not perfectly aligned along the [001] axis below T_M. Our results show that the spin alignment above the Morin transition can also be imperfect, with the spins rotated away from the (001) plane by a significant angle.

All of the samples investigated in this work have impurities of magnetite in amounts that give rise to visible diffraction peaks but that except for the hem sample are not detectible by Mössbauer spectroscopy due to overlapping lines. While the magnetite impurities are likely to be important for the macroscopic magnetic properties of the sample (the bulk magnetization) inclusions of magnetite in the structure may not be important for the spin structure in the hematite-ilmenite phase. Other impurities or defects may, however, be important for the spin orientation and could explain the variation in spin angle between samples.

It may seem surprising that we find a significant out-of-plane spin component in hematite but it is consistent with the experiments of Parise et al. (2006) and Klotz et al. (2013). While our sample is a natural sample, which contains impurities that could affect its magnetic structure, the samples investigated by both Parise et al. (2006) and Klotz et al. (2013) were high purity synthetic samples and impurities are thus unlikely to be the sole cause of the observations of out-of-plane spin orientation in hematite. Klotz et al. (2013) ascribe the spin orientation as an artifact of the Rietveld method's insensibility to changes in α. It is true that the quality of the Rietveld-fit, as quantified by the χ^2- value or any other measure of the sum of residuals, does not depend strongly on the spin orientation but it is clear that the model with $\alpha = 20.0°$ (close to the refined value $\alpha = 18.1°$) represents the data much better than $\alpha = 0°$, as can be seen in Figure 9, where the (101) and (003) magnetic peaks at room temperature are plotted together with models with different

values of α. However, the insensitivity of the fit to variations in α, when α is close to 0° has the consequence that the experiment becomes very susceptible to systematic errors. We have not identified any systematic errors in this experiment that could give rise to the observed out-of-plane spin orientation.

The insensitivity to variations in the spin angle is not unique to the Rietveld method, but is a consequence of the small change in $1 - \sin^2(\alpha)$ (which is essentially the measured quantity) when α is small. To completely eliminate this problem one would have to perform a polarized neutron diffraction experiment on a single crystal of hematite.

We have studied the spin orientation in synthetic samples of hematite-ilmenite as well as a natural sample of hematite with neutron powder diffraction and Mössbauer spectroscopy. We find that the spin has a significant component out of the basal plane in all samples. The nonzero tilt-angle of the antiferromagnetic sublattices is consistent with other studies but we cannot at present give a detailed explanation of the origin of this deviation from the usually assumed magnetic structure with the spins confined to the basal plane. The tilt angles in our samples are in the range 11.0 (9)° - 22.7 (5)°, and seem not to depend systematically on Ti-content. Furthermore, the out-of-plane angle does not require an exsolution structure as seen in natural samples.

Implications

The implications of the present results cannot be appreciated without going back to the theoretical paper on hematite magnetization by Dzyaloshinsky (1958). This showed both the individual layer spin orientations and the spin-canted ferromagnetic moments parallel to the (001) crystallographic plane. This understanding persisted for the next half century and was enshrined in the major book "Canted Antiferromagnetism" by Morrish (1994). The first warnings that this might be incorrect came from Monte Carlo modeling of low-temperature giant magnetic exchange bias in

titanohematite with nanoscale ilmenite exsolution lamellae (Harrison et al. 2007), and evidence that such exchange bias could be produced when similar natural samples were cooled in zero field to low temperature before the hysteresis experiment (Fabian et al. 2008). These studies implied that an unexpected out-of-plane component of spin should exist in the hematite, even at room temperature and above. This was later observed directly in a similar exsolved sample (Harrison et al. 2010), but was then attributed to a localized effect of Fe^{2+} cations at interfaces. The present results indicate instead, for the first time, that the out-of-plane spin component is an intrinsic feature of hematite itself, with an origin not yet fully understood, but consistent with group theory. Probably earlier workers mistook the crystallographic position of the spin-canted ferromagnetic moment as also the position of the individual layer spin components. The present work thus establishes a major shift in understanding of one of the two mineral systems responsible for rock magnetism.

Acknowledgments

The neutron experiments were performed at ISIS, Oxfordshire, UK and Institut Max von Laue Paul Langevin, Grenoble, France. This work was supported by the Danish Agency for Science, Technology and Innovation through DanScatt. The research leading to these results has received funding from the European Research Council under the European Union's Seventh Framework Programme (FP/2007-2013) ERC grant agreement 320750. The authors acknowledges the assistance of Aziz Daoud-Aladine during the experiments at ISIS.

References

Artman, J.O., Muir, A.H., and Wiedersich, H. (1968) Determination of the nuclear quadrupole moment of Fe^{57m} from α-Fe_2O_3 data. Physical Review, 173, 337.

Artman, J.O., Murphy, C.J., and Foner, S. (1965) Magnetic anisotropy in antiferromagnetic corundum-type sesquioxides. Physical Review, 138, 3A, A912.

Besser, P.J., Morrish, A.H., and Searle, C.W. (1967) Magnetocrystalline anisotropy of pure and doped hematite. Physical Review, 153, 632-642.

Burton, B. P., Robinson, P., McEnroe, S. A., Fabian, K., and Boffa Ballaran, T. (2008) A low-temperature phase diagram for ilmenite-rich compositions in the system Fe_2O_3-$FeTiO_3$. American Mineralogist, 93, 1260-1272.

Butler, W. H., Bandyopadhyat, A., and Srinivasan, R. (2003) Electronic and magnetic structure of a 1000 K magnetic semiconductor: α-hematite (Ti). Journal of Applied Physics, 93, 7882.

Brok, E., Sales, M., Lefmann, K., Theil Kuhn, L., Schmidt, W.F., Roessli, B., Robinson, P., McEnroe, S.A., Harrison, R.J. (2014) Experimental evidence for lamellar magnetism in hemo-ilmenite by polarized neutron scattering, Physical Review B., 89, 054430.

Bødker, F., Hansen, M.F., Koch, C.B., Lefmann, K, and Mørup, S (2000) Magnetic properties of hematite nanoparticles. Physical Review B, 61, 10, 6826-6838.

Dzyaloshinsky, I. (1958). A Thermodynamic theory of "weak" ferromagnetism of antiferromagnetics. Journal of Physics and Chemistry of Solids, 4, 241-255.

Fabian, K., McEnroe, S.A., Robinson P., and Shcherbakov, V.P. (2008) Exchange bias identifies lamellar magnetism as the origin of the natural remanent magnetization in titanohematite with ilmenite exsolution from Modum, Norway. Earth and Planetary Science Letters, 268, 339.

Fabian, K., Miyajima, N., Robinson, P., McEnroe, S.A., Ballaran, T., and Burton, B.P. (2011) Chemical and magnetic properties of rapidly cooled metastable ferri-ilmenite solid solutions: implications for magnetic self-reversal and exchange bias, I. Fe-Ti order transition in quenched synthetic ilmenite 61. Geophys. J. Int. 186, 997–1014

Flanders, P.J., (1972) Observation of a c-axis moment in α-Fe_2O_3. Journal of Applied Physics, 43, 2430-2435.

Frandsen, C., Burton, B.P., Rasmussen, H.K., McEnroe, S.A., and Mørup S. (2010) Magnetic clusters in ilmenite-hematite solid solutions. Physical Review B, 81, 224423.

Frandsen, C., Lefmann, K., Lebech, B., Bahl, C.R.H., Brok, E., Ancoña, S.N., Theil Kuhn, L., Keller, L., Kasama, T., Gontard, L.C., and Mørup S. (2011) Spin reorientation in α-Fe_2O_3 induced by interparticle exchange interactions in α-Fe_2O_3/NiO nanocomposites. Physical Review B, 84, 214435.

Fujii, T., Kayano, M., Takada, Y., Nakanishi, M., and Takada, J. (2004) Ilmenite-hematite solid solution films for novel electronic devices. Solid State Ionics, 172, 289-292.

Harrison, R.J., and Redfern S.A.T. (2001) Short- and long-range ordering in the ilmenite-hematite solid solution. Physical Chemistry of Minerals, 28, 399-412.

Harrison, R.J., McEnroe, S.A., Robinson, P., Carter-Stiglitz, B., Palin, E.J., and Kasama, T. (2007) Low-temperature exchange coupling between Fe_2O_3 and $FeTiO_3$: Insight into the mechanism of giant exchange bias in a natural nanoscale intergrowth. Physical Review B, 76, 174436.

Harrison, R.J., McEnroe, S.A., Robinson, P., and Howard, C.J. (2010) Spin orientation in a natural Ti-bearing hematite: Evidence for an out-of-plane component. American Mineralogist, 95, 974.

Ishikawa, Y., and Akimoto, S. (1957) Magnetic properties of the FeTiO3-Fe2O3 solid solution series. Journal of the Physical Society of Japan, 12, 1083-1098.

Ishikawa, Y. (1958) Electrical properties of FeTiO3-Fe2O3 solid solution series. Journal of the

Physical Society of Japan, 13, 37-42.

Kletetschka, G., Wasilewski, P.J., and Taylor, P.T. (2002) The role of hematite-ilmenite solid solution in the production of magnetic anomalies in ground- and satellite-based data. Tectonophysics, 347, 167.

Klotz, S., Strässle, Th. And Hansen Th. (2013) Pressure dependence of Morin transition in α-Fe_2O_3 hematite. Europysicsletters 104, 16001.

Krén, E., Molnàr, B., Svàb, E., and Zsoldos, E. (1974) Neutron Diffraction Study of the (1-x)Fe_2O_3-xAl_2O_3 System. Solid State Communications, 15, 1707-1710.

Larson, A.C. and von Dreele, R.B. (1994) General Structure Analysis System (GSAS). Los Alamos National Laboratory Report LAUR 86-748.

McEnroe, S.A., Robinson, P., and Panish, P.T. (2001) Aeromagnetic anomalies, magnetic petrology, and rock magnetism of hemo-ilmenite- and magnetite-rich cumulate rocks from the Sokndal region, South Rogaland, Norway. American Mineralogist, 86, 1447.

McEnroe, S.A., Harrison, R.J., Robinson, P., and Langenhorst, F. (2002) Nanoscale haematite-ilmenite lamellae in massive ilmenite rock: an example of 'lamellar magnetism' with implications for planetary magnetic anomalies. Geophysical Journal International, 151, 890-912.

McEnroe, S.A., Skilbrei, J.R., Robinson, P., Heidelbach, F., and Langenhorst, F. (2004) Magnetic anomalies, layered intrusions and Mars. Geophysical Research Letters, 31, L19601.

McEnroe, S.A., Carter-Stiglitz, B., Harrison, R.J., Robinson, P., Fabian, K., and McCammon, C. (2007) Magnetic exchange bias of more than 1 tesla in a natural mineral intergrowth. Nature Nanotechnology, 2, 631.

Morin, F.J. (1950) Magnetic susceptibility of αFe_2O_3 and αFe_2O_3 with added titanium. Physical Review, 78, 819-820.

Morrish, A.H. (1994) Canted Antiferromagnetism: Hematite, World Scientific, Singapore.

Morrish, A.H., Johnston, G.B., and Curry, N.A. (1963) Magnetic transition in pure and Ga doped α-Fe_2O_3. Physics Letters, 7, 3, 177.

Parise, J.B., and Locke, D.R., Tulk, C.A., Swainson, I., and Cranswick, L. (2006) The effect of pressure on the Morin transition in hematite (alpha-Fe_2O_3). Physica B – Condensed Matter, 385, 391.

Robinson, P., Harrison, R.J., McEnroe S.A., and Hargreaves, R.B. (2002) Lamellar magnetism in the haematite-ilmenite series as an explanation for strong remanent magnetization. Nature, 418, 517.

Robinson, P., Harrison, R.J., McEnroe S.A., and Hargreaves, R.B. (2004) Nature and origin of lamellar magnetism in the hematite-ilmenite series. American Mineralogist, 89, 725-747.

Robinson, P., Harrison, R.J., Myajima, N., McEnroe, S.A., and Fabian K. (2011) Chemical and magnetic properties of rapidly cooled metastable ferri-ilmenite solid solutions: implications for magnetic self-reversal and exchange bias, II. Chemical changes during quench and annealing. Geopysical Journal International, 188, 447-472.

Robinson, P, Harrison, R.J., Fabian, K., and McEnroe, S.A. (2012) Chemical and magnetic properties of rapidly cooled metastable ferri-ilmenite solid solutions: implications for magnetic self-reversal and exchange bias, III. Magnetic interactions in samples produced by Fe-Ti ordering. Geophysical Journal International, 191, 1025-1047.

Robinson, P, McEnroe, S.A., Fabian, K., Harrison, R.J., Thomas, C.I. and Mukai, H. (2014) Chemical and magnetic properties of rapidly cooled metastable ferri-ilmenite solid solutions - IV. The fine structure of self-reveres thermoremanent magnetization. Geophysical Journal International, 196, 1375-1396.

Shull, C.G., Strauser, W.A., and Wollan, E. (1951) Neutron diffraction by paramagnetic and antiferromagnetic substances. Physical Review, 83, 333-345.

Sváb, E., and Krén, E. (1979) Neutron diffraction study of substituted hematite. Journal of Magnetism and Magnetic Materials, 14, 184-186.

Vandenberghe, R. E., Van San, E., De Grave, E. (2001) About the Morin transition in hematite in relation with particle size and aluminium substitution. Czech. J. Phys., 51, 7, 663-675.

Vandenberghe, R. E., Van San, E., De Grave, E. (2002) Evidence of intermediate magnetic states in non-stoichiometric hematite. Hyperfine Int. C5, 209-212.

List of Figure captions

Figure 1. Crystal and magnetic structure between T_M and T_N. The large balls are O atoms and the smaller balls are Fe (or substituted Ti) atoms. The arrows indicate the spin orientation with a 20° tilt away from the basal plane.

Figure 2. Room temperature neutron powder diffraction patterns. (a) Ilm13 measured at D20. (b) Hem measured at OSIRIS. The uncertainty (σ) is smaller than the size of the points.

Figure 3. Representation of the set of diffraction patterns of ilm13 measured at D20. The two lines at $d \approx 4.2$ Å and $d \approx 4.6$ Å are the hematite (101) and (003) magnetic peaks. The weak lines that gain in intensity at temperatures above 1000 K are from the magnetite structure.

Figure 4. Refined in-plane ($M_{\parallel}$), out-of-plane ($M_{\perp}$) and total (M_{tot}) moment as a function of temperature for samples hem, ilm13, ilm20 and ilm35. The solid lines are power law fits. The error bars represent one standard deviation (σ).

Figure 5. Left: Total magnetic moment as function of the reduced temperature. The solid lines are the same fits as in Fig. 3. Right: Out-of-plane tilt-angle α as function of the reduced temperature. The ilm13 data has been binned so that each data point represents a 17 K temperature interval. The error bars represent one standard deviation (σ).

Figure 6. Out-of-plane vs. in-plane moment. The lines are linear fits to the blue data points. The error bars represent one standard deviation (σ).

Figure 7. Lattice parameters as function of temperature. The dashed vertical lines mark T_N = 799.9 K. The data has been binned so that each data point represents a 17 K temperature interval. The uncertainty (σ) is smaller than the size of the points.

Figure 8. The crystallographic β_m angle as a function of temperature. The dashed vertical line marks T_N = 799.9 K. The data has been binned so that each data point represents a 17 K temperature interval. The error bars represent one standard deviation (σ).

Figure 9. Room temperature Mössbauer spectra of hem, ilm20, ilm35 and ilm40. The blue lines are the fits described in the text. The hem data is fitted well with a single sextet for hematite plus 2 sextets for magnetite (black). The spectra of the Ti-containing samples are fitted with 4 sextets (green) and for the ilm35 sample a small doublet component is added to the fit. The measurement uncertainty (σ) is smaller than the size of the points.

Figure 10. Refinement of the room temperature hem data at a reduced *d*-spacing range 4.015 Å – 4.708 Å with different fixed values of α. Only the magnitude of the magnetic moment and 3 background parameters are refined and the remaining parameters are fixed at the values from the refinement of room temperature diffraction pattern in the entire experimental *d*-spacing range. The size of the refined magnetic moment does not deviate significantly from 4.21(2) μ_B when α is changed, except when α=30° where the total moment decreases to 4.01(3) μ_B.

	V (Å^3)	x	$M_{\parallel}$ (μ_B)	$M_{\perp}$ (μ_B)	M_{tot} (μ_B)	α (°)
hem	301.41 (3)	0	4.00 (3)	1.31 (4)	4.21 (2)	18.1 (6)
ilm13	303.69 (3)	0.176 (12)	3.98 (10)	0.80 (12)	4.06 (5)	11 (2)
Ilm20	304.05 (4)	0.207 (10)	3.81 (4)	1.21 (6)	4.00 (2)	17.6 (9)
Ilm35	305.62 (4)	0.341 (10)	3.24 (2)	1.36 (3)	3.51 (2)	22.7 (5)
Ilm40	306.18 (4)	0.387 (10)	3.45 (4)	1.17 (5)	3.64 (2)	18.7 (9)

Table 1: Unit cell volume, composition, magnetic moment, and spin-angle from refinement of room temperature data (ilm35 was actually measured at 50 °C). The compositions were determined from the unit cell volume using Equation 1.

	hem	**Ilm13**	**Ilm20**	**Ilm35**	**Ilm40**
T_N **(K)**	948.8 (4)	799.9 (7)	760 (6)	676.3 (4)	606.4 (12)

Table 2: Néel temperatures determined from power law fit of M_{tot}.

		Sextet 1	Sextet 2	Sextet 3	Sextet 4
hem	B_{hf} (T)	51.50			
	IS (mm/s)	0.370			
	ε (mm/s)	-0.094			
	Area (%)	90.0			
Ilm20	B_{hf} (T)	50.23	48.96	47.45	44.61
	IS (mm/s)	0.384	0.397	0.422	0.523
	ε (mm/s)	-0.105	-0.100	-0.078	-0.035
	Area (%)	32.2	27.1	18.9	21.8
Ilm35	B_{hf} (T)	48.77	47.21	45.07	39.27
	IS (mm/s)	0.393	0.400	0.449	0.642
	ε (mm/s)	-0.110	-0.098	-0.076	-0.021
	Area (%)	23.2	22.6	24.5	27.2

Ilm40	B_{hf} (T)	48.14	46.45	43.77	37.23
	IS (mm/s)	0.393	0.419	0.471	0.670
	ε (mm/s)	-0.108	-0.099	-0.077	-0.009
	Area (%)	15.2	24.2	26.8	33.7

Table 3: Fit parameters, hyperfine field (B_{hf}), isomer shift (*IS*), quadrupole shift (ε) and relative spectral area from sextet fit to room temperature Mössbauer data. The uncertainty on the fitted B_{hf} is approximately 0.02 T and the uncertainty on *IS* and ε 0.004 mm/s. The reason the spectral areas for hem and ilm35 does not sum to 100 % is the magnetite component in hem which takes up 10 % of the spectral area, and the central doublet in ilm35, which takes up a spectral area of 2.6%.

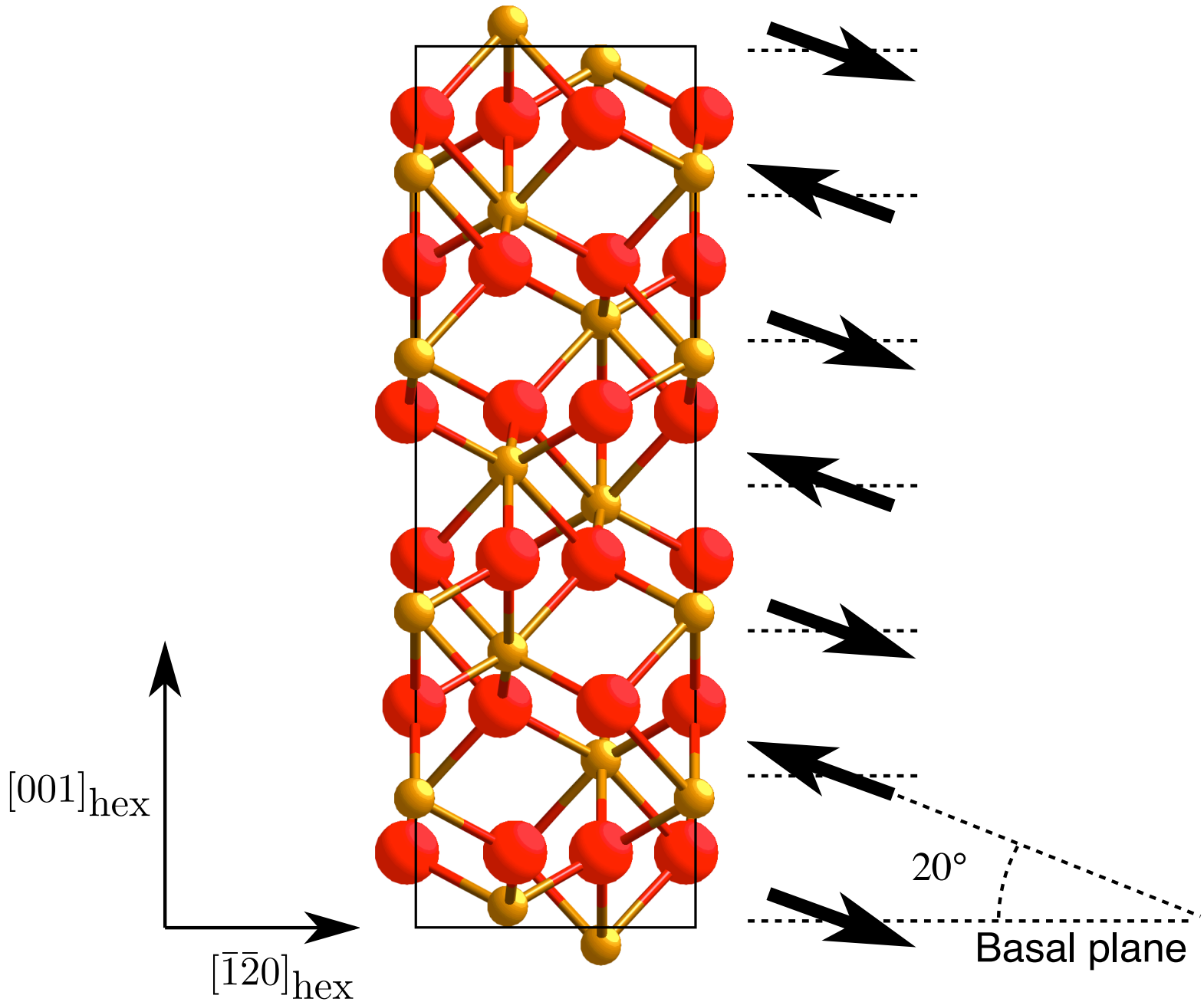

This is a preprint, the final version is subject to change, of the American Mineralogist (MSA)
Cite as Authors (Year) Title. American Mineralogist, in press.
(DOI will not work until issue is live.) DOI: http://dx.doi.org/10.2138/am-2017-5792CCBY

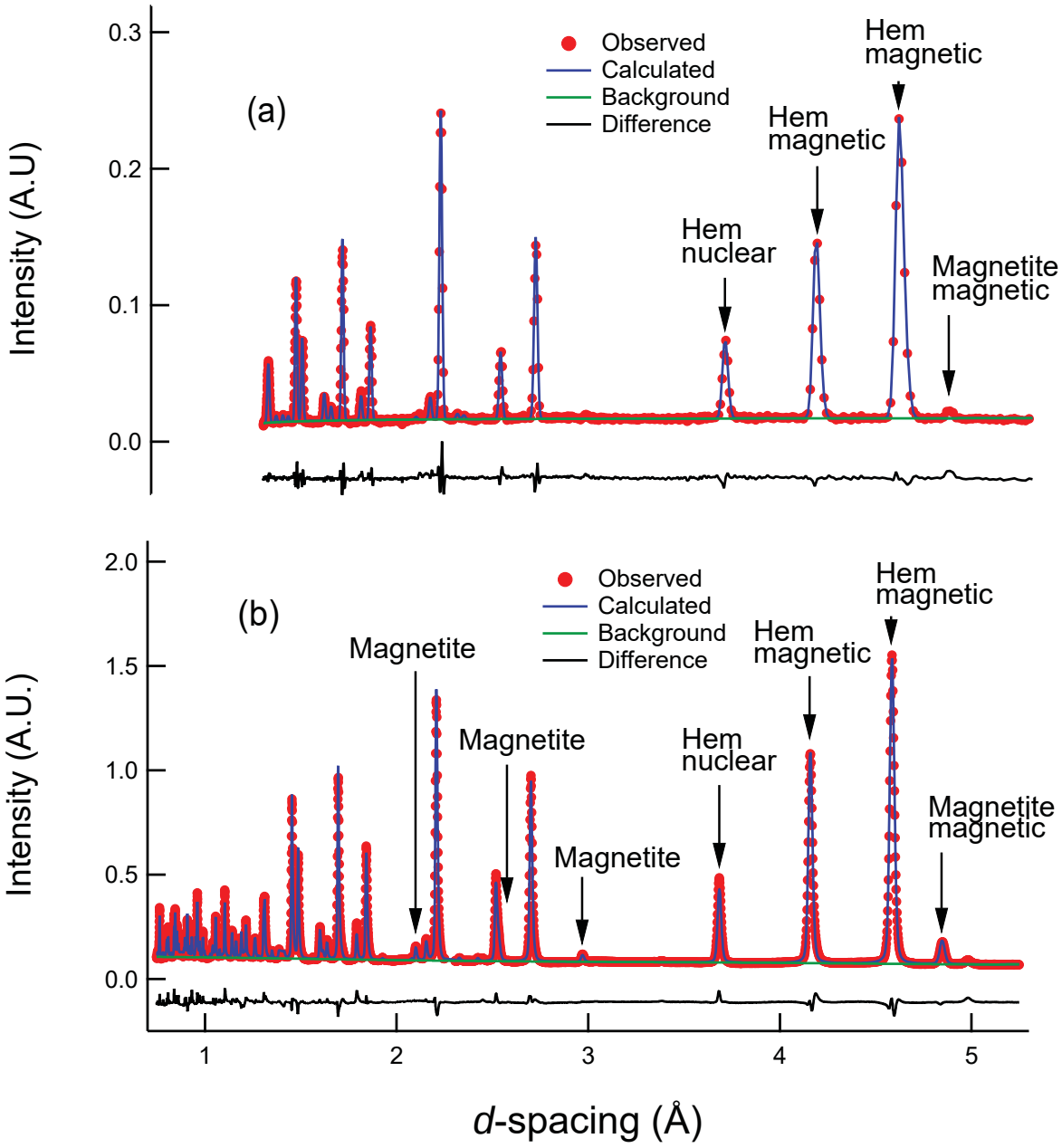

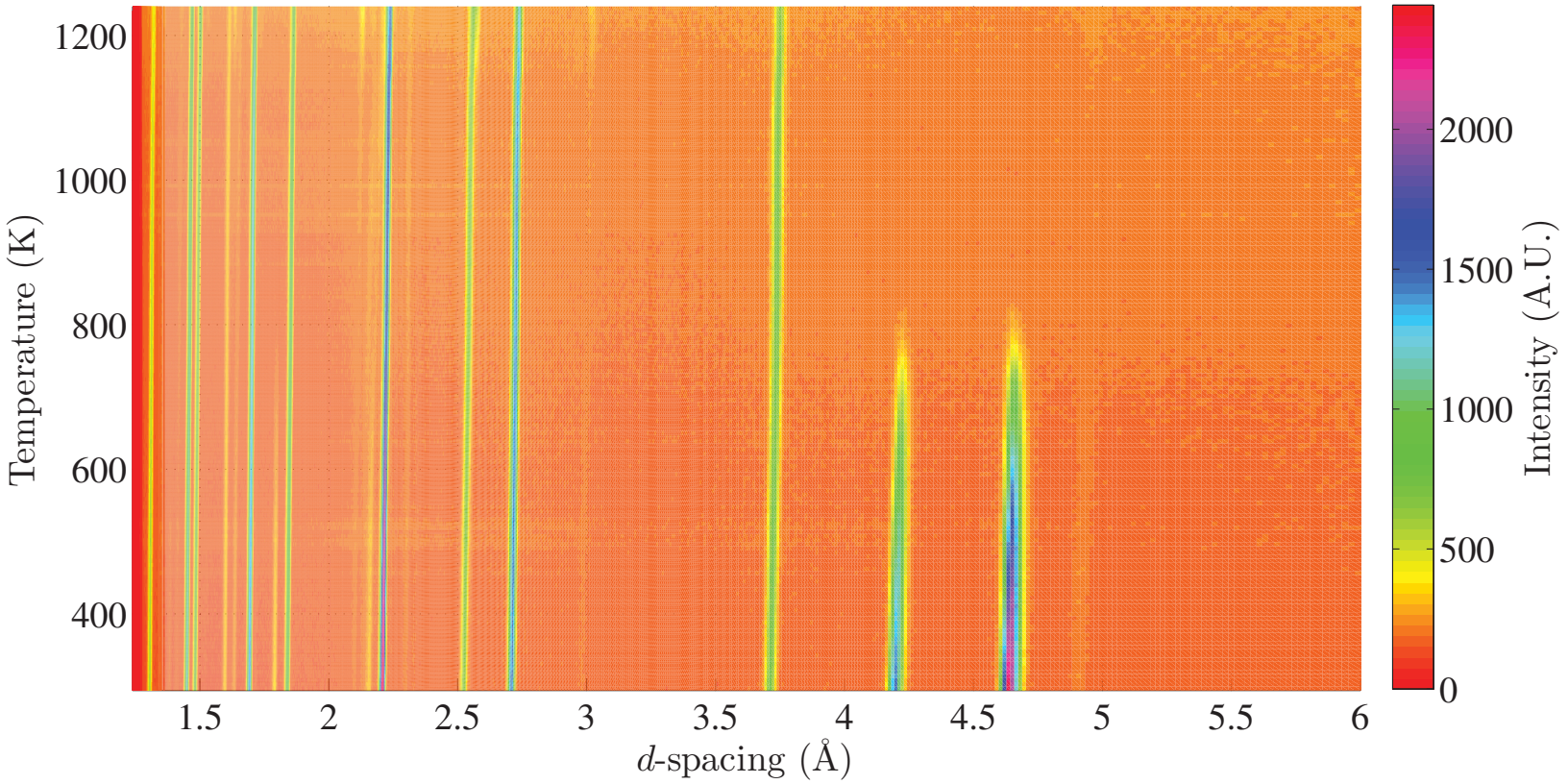

This is a preprint, the final version is subject to change, of the American Mineralogist (MSA)
Cite as Authors (Year) Title. American Mineralogist, in press.
(DOI will not work until issue is live.) DOI: http://dx.doi.org/10.2138/am-2017-5792CCBY

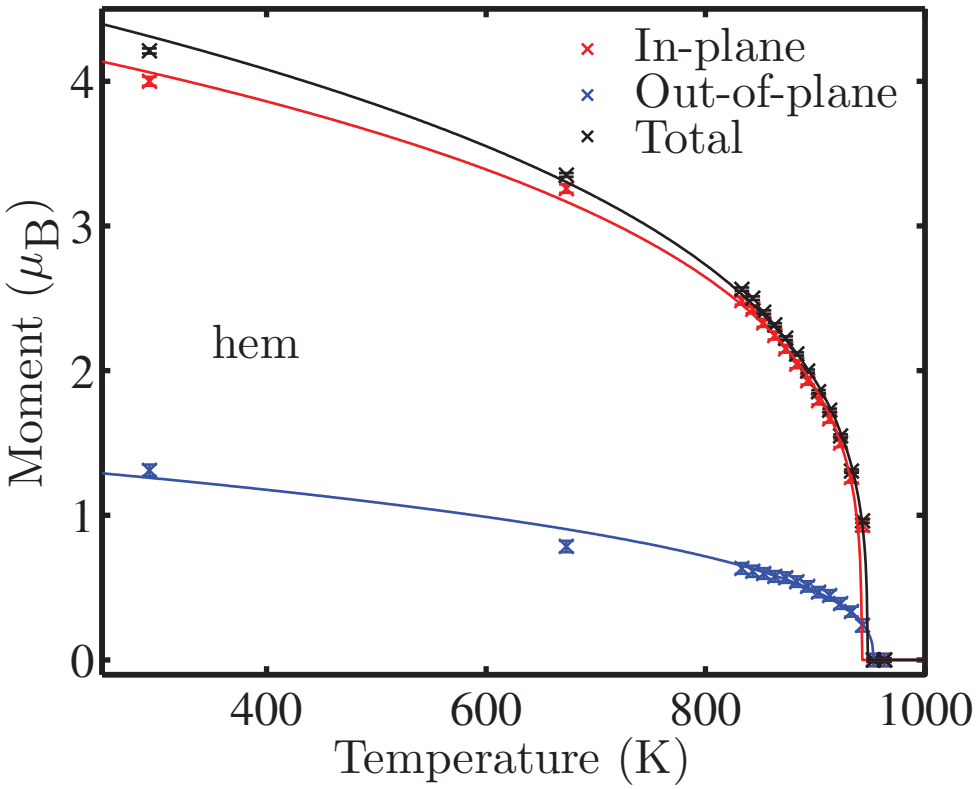

This is a preprint, the final version is subject to change, of the American Mineralogist (MSA)
Cite as Authors (Year) Title. American Mineralogist, in press.
(DOI will not work until issue is live.) DOI: http://dx.doi.org/10.2138/am-2017-5792CCBY

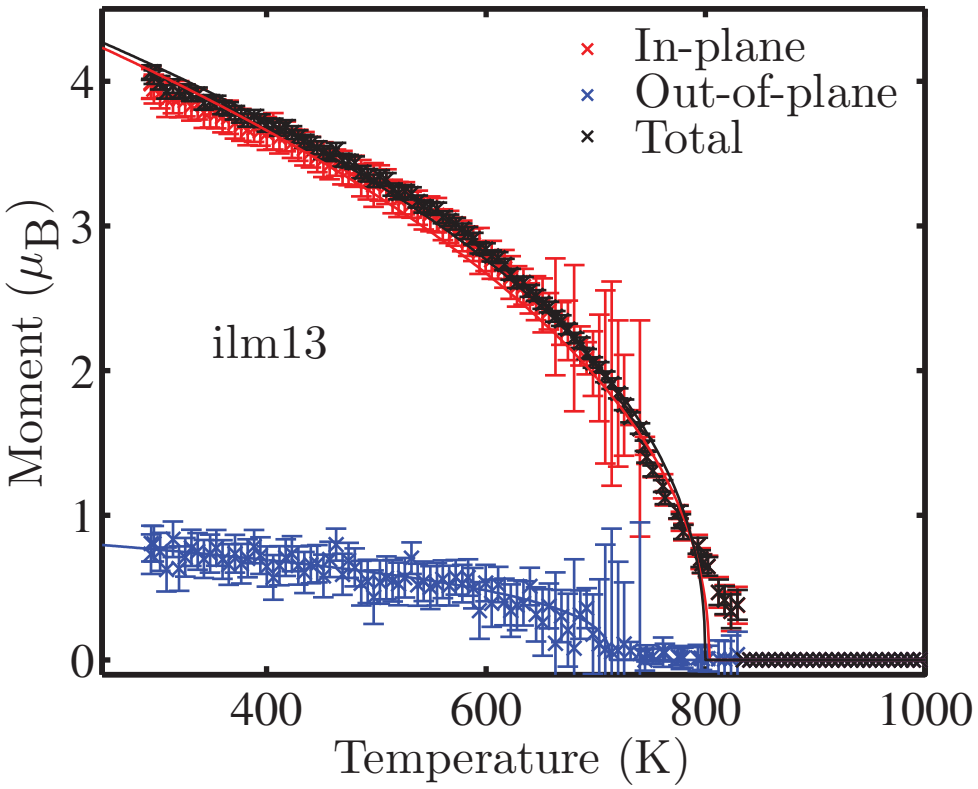

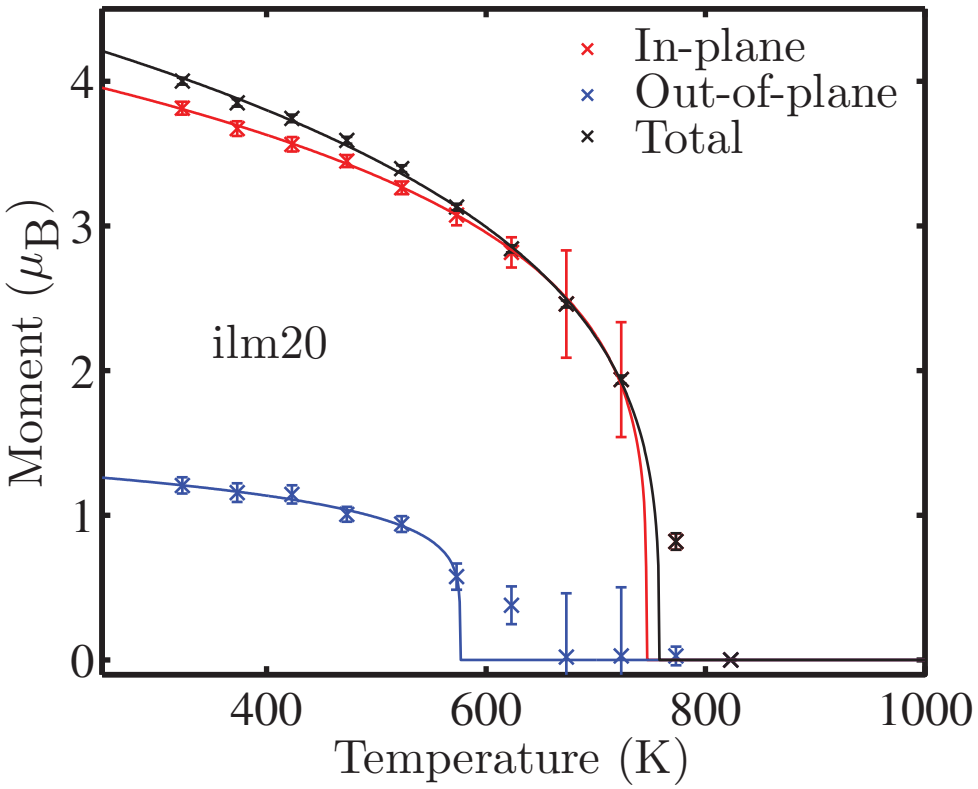

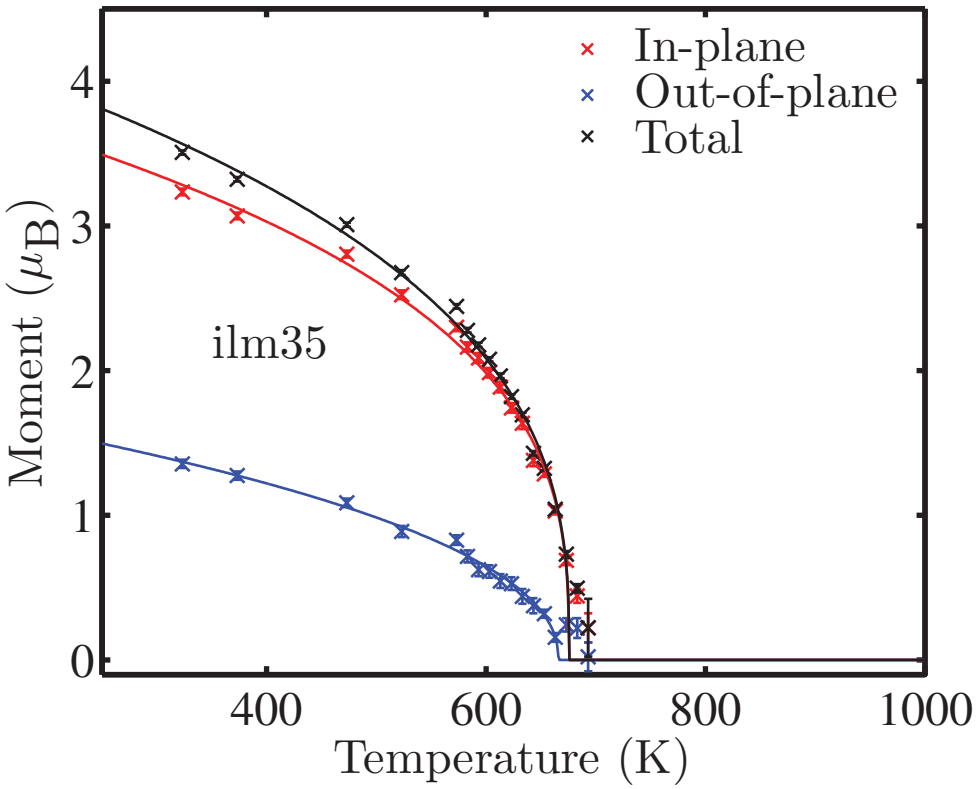

This is a preprint, the final version is subject to change, of the American Mineralogist (MSA)
Cite as Authors (Year) Title. American Mineralogist, in press.
(DOI will not work until issue is live.) DOI: http://dx.doi.org/10.2138/am-2017-5792CCBY

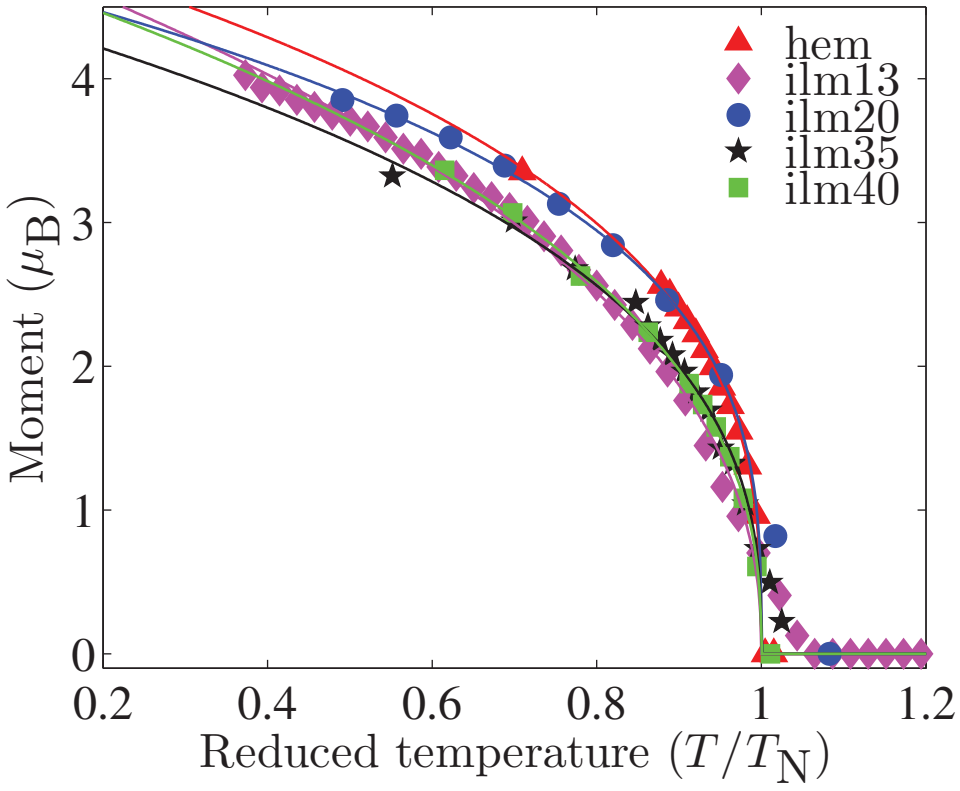

This is a preprint, the final version is subject to change, of the American Mineralogist (MSA)
Cite as Authors (Year) Title. American Mineralogist, in press.
(DOI will not work until issue is live.) DOI: http://dx.doi.org/10.2138/am-2017-5792CCBY

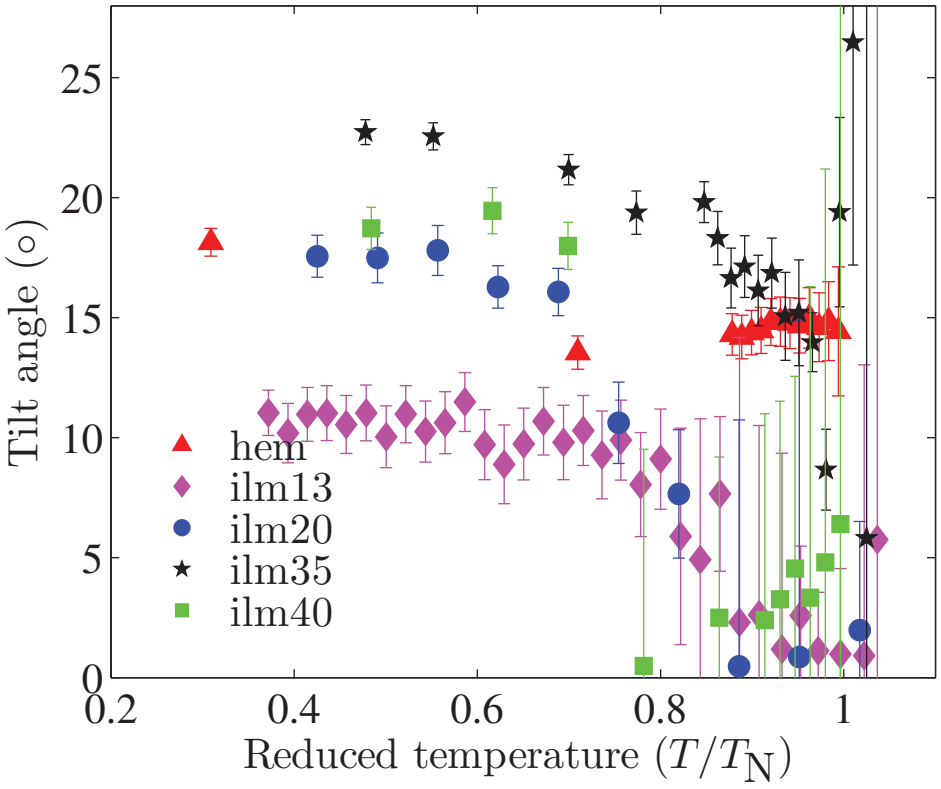

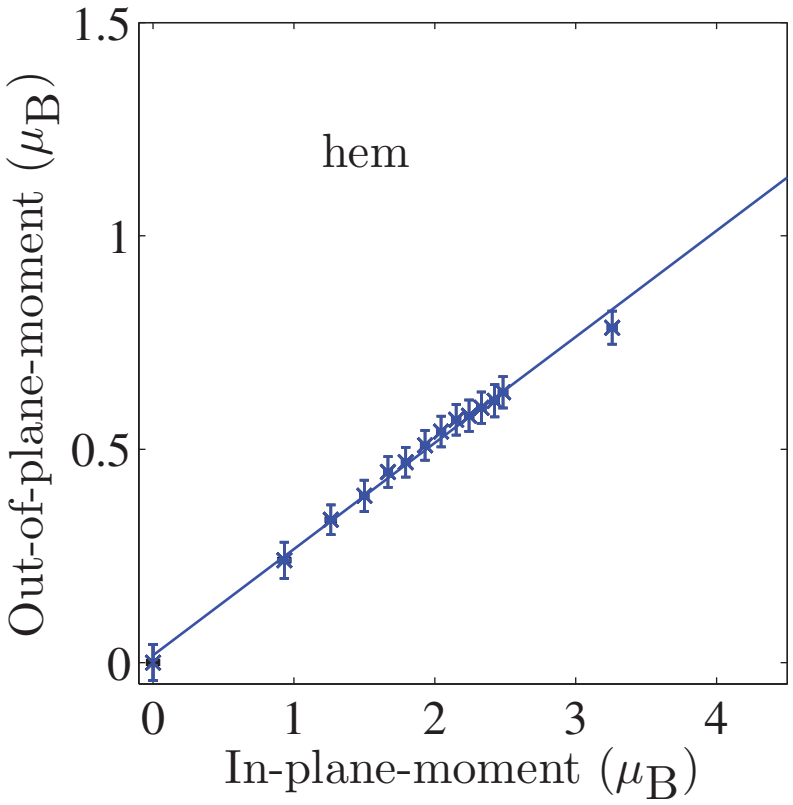

This is a preprint, the final version is subject to change, of the American Mineralogist (MSA)
Cite as Authors (Year) Title. American Mineralogist, in press.
(DOI will not work until issue is live.) DOI: http://dx.doi.org/10.2138/am-2017-5792CCBY

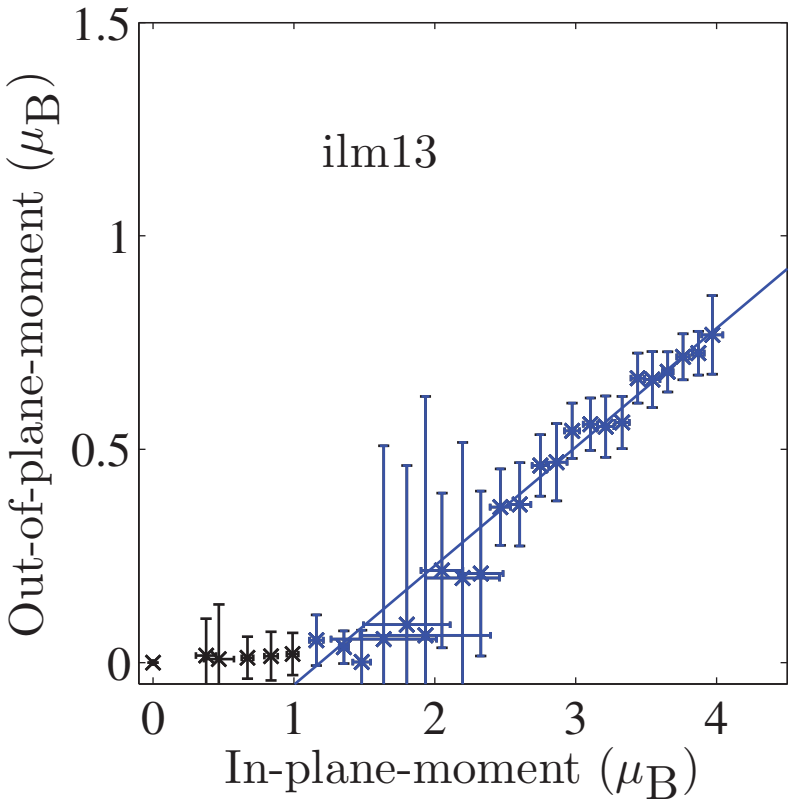

This is a preprint, the final version is subject to change, of the American Mineralogist (MSA)
Cite as Authors (Year) Title. American Mineralogist, in press.
(DOI will not work until issue is live.) DOI: http://dx.doi.org/10.2138/am-2017-5792CCBY

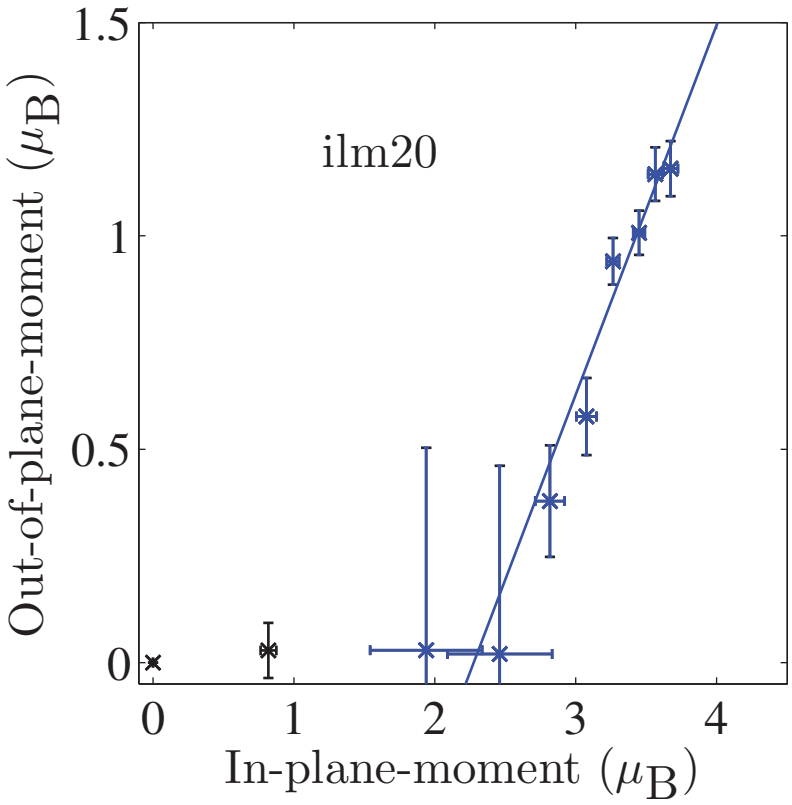

This is a preprint, the final version is subject to change, of the American Mineralogist (MSA)
Cite as Authors (Year) Title. American Mineralogist, in press.
(DOI will not work until issue is live.) DOI: http://dx.doi.org/10.2138/am-2017-5792CCBY

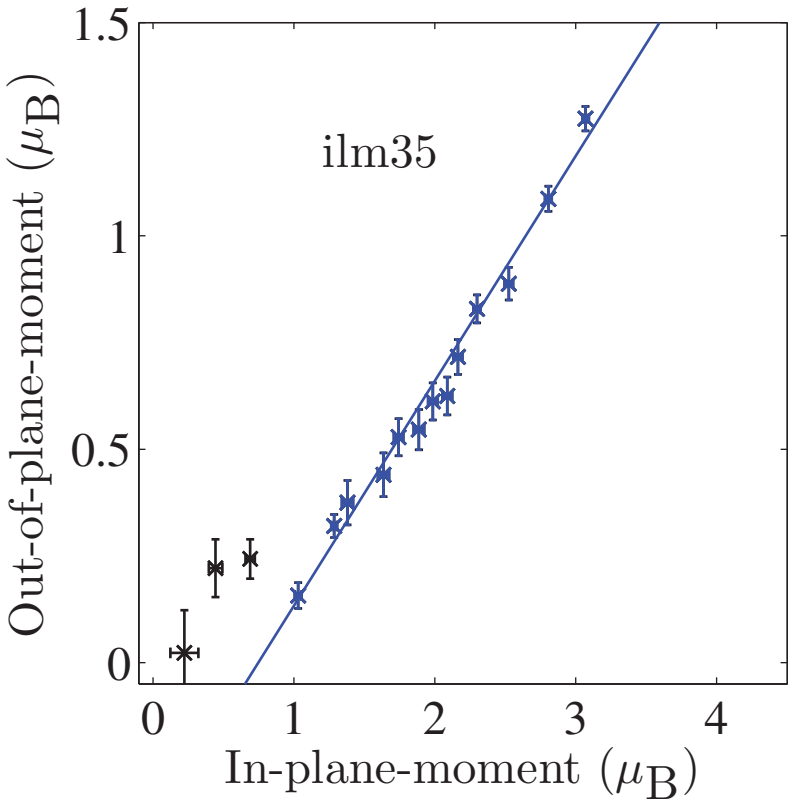

This is a preprint, the final version is subject to change, of the American Mineralogist (MSA)
Cite as Authors (Year) Title. American Mineralogist, in press.
(DOI will not work until issue is live.) DOI: http://dx.doi.org/10.2138/am-2017-5792CCBY

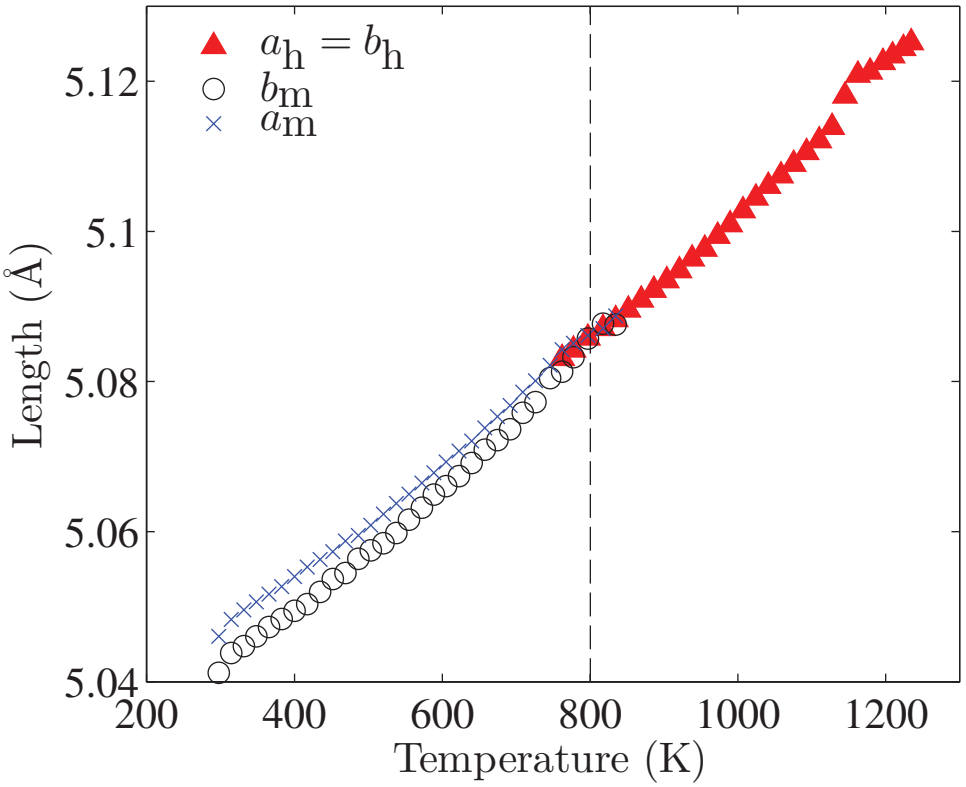

This is a preprint, the final version is subject to change, of the American Mineralogist (MSA)
Cite as Authors (Year) Title. American Mineralogist, in press.
(DOI will not work until issue is live.) DOI: http://dx.doi.org/10.2138/am-2017-5792CCBY

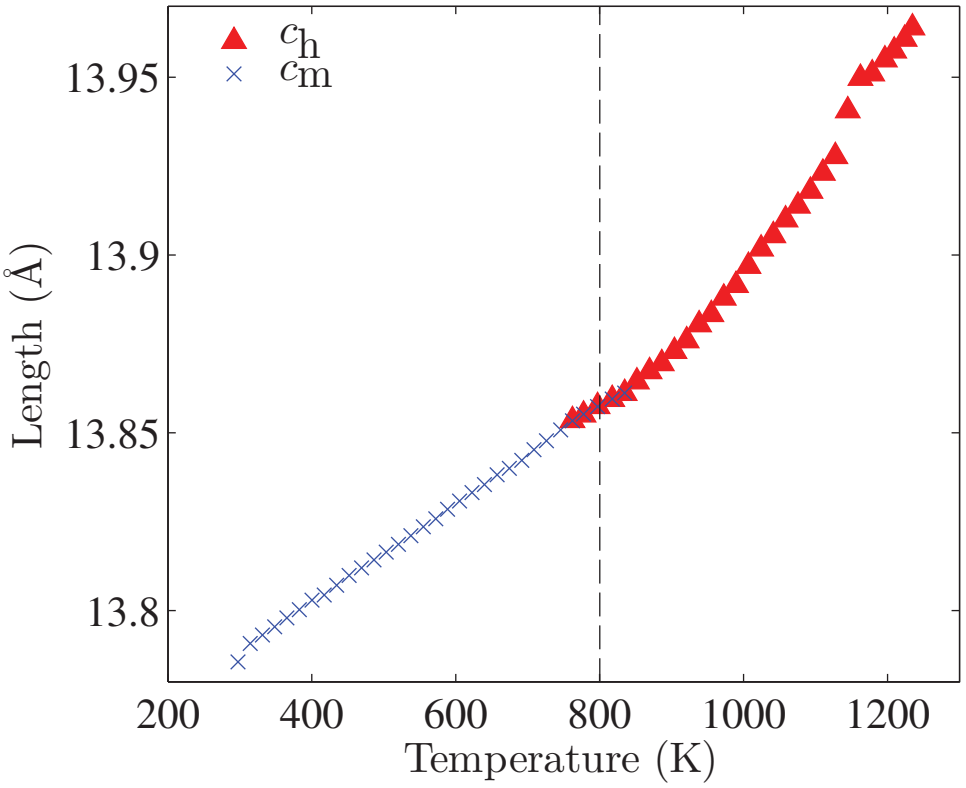

This is a preprint, the final version is subject to change, of the American Mineralogist (MSA)
Cite as Authors (Year) Title. American Mineralogist, in press.
(DOI will not work until issue is live.) DOI: http://dx.doi.org/10.2138/am-2017-5792CCBY